OXFORD

SOT | Society of Toxicology
www.toxsci.oxfordjournals.org

TOXICOLOGICAL SCIENCES, 171(1), 2019, 69–83

doi: 10.1093/toxsci/kfz134
Advance Access Publication Date: June 19, 2019
Research Article

Physiologically Based Kinetic Modeling-Facilitated Reverse Dosimetry to Predict *In Vivo* Red Blood Cell Acetylcholinesterase Inhibition Following Exposure to Chlorpyrifos in the Caucasian and Chinese Population

Shensheng Zhao,*,[1] Lenny Kamelia,* Rungnapa Boonpawa,† Sebastiaan Wesseling,* Bert Spenkelink,* and Ivonne M.C.M. Rietjens*

*Division of Toxicology, Wageningen University and Research, Wageningen, The Netherlands; and †Faculty of Natural Resources and Agro-Industry, Kasetsart University Chalermphrakiat Sakon Nakhon Province Campus, Thailand

[1]To whom correspondence should be addressed at Division of Toxicology, Wageningen University and Research, PO BOX 8000, 6708 EA Wageningen, The Netherlands. Fax: +31(0)317484931. E-mail: shensheng.zhao@wur.nl.

ABSTRACT

Organophosphates have a long history of use as insecticides over the world. The aim of the present study was to investigate the interethnic differences in kinetics, biomarker formation, and *in vivo* red blood cell acetylcholinesterase inhibition of chlorpyrifos (CPF) in the Chinese and the Caucasian population. To this purpose, physiologically based kinetic models for CPF in both the Chinese and Caucasian population were developed, and used to study time- and dose-dependent interethnic variation in urinary biomarkers and to convert concentration-response curves for red blood cell acetylcholinesterase inhibition to *in vivo* dose-response curves in these 2 populations by reverse dosimetry. The results obtained revealed a marked interethnic difference in toxicokinetics of CPF, with lower urinary biomarker levels at similar dose levels and slower CPF bioactivation and faster chlorpyrifos-oxon detoxification in the Chinese compared with the Caucasian population, resulting in 5- to 6-fold higher CPF sensitivity of the Caucasian than the Chinese population. These differences might be related to variation in the frequency of single-nucleotide polymorphisms for the major biotransformation enzymes involved. To conclude, the interethnic variation in kinetics of CPF may affect both its biomarker-based exposure assessment and its toxicity and risk assessment and physiologically based kinetic modeling facilitates the characterization and quantification of these interethnic variations.

Key words: organophosphate pesticide; chlorpyrifos; interethnic variation; physiologically based kinetic modeling; reverse dosimetry; acetylcholinesterase inhibition.

Organophosphate pesticides (OPs) are an important class of crop protection agents used worldwide (Stauber *et al.*, 2016). OPs and their metabolites have been detected in human urine, blood, serum, and breast milk (Drevenkar *et al.*, 1994; Hardt and Angerer, 2000; Liu et al., 2014; Naksen *et al.*, 2016; Zhang *et al.*, 2014), reflecting human exposure to these pesticides. Upon acute exposure, the activated form of OPs can covalently bind to and inhibit acetylcholinesterase (AChE), the enzyme responsible for hydrolysis of the neurotransmitter acetylcholine (ACh) (Flaskos, 2014). This inhibition causes accumulation of ACh in the synaptic cleft, resulting in overstimulation of the ACh receptor ultimately causing cholinergic dysfunction, paralysis, and

respiratory failure (Eaton *et al.*, 2008; Hung *et al.*, 2015). Chronic low dose exposure to OPs has been associated with poorer neurobehavioral development in infants/school children and poorer intellectual development in 7-year-old children (Bouchard *et al.*, 2011; González-Alzaga *et al.*, 2014; Wang *et al.*, 2012).

In the past decades, physiologically based kinetic (PBK) models have been developed for a few OPs, i.e. chlorpyrifos (CPF) (Bouchard *et al.*, 2005; Lu et al., 2009; Mosquin *et al.*, 2009; Timchalk *et al.*, 2002) and diazinon (Poet *et al.*, 2004), in order to better predict the internal exposure level and risk upon exposure to OPs (Bouchard *et al.*, 2005; Foxenberg *et al.*, 2011; Lu et al., 2009; Mosquin *et al.*, 2009; Nolan *et al.*, 1984; Timchalk *et al.*, 2002). These PBK models can be used for reverse dosimetry, enabling translation of urinary biomarker data to internal or external exposure levels, whereas in theory, also enabling conversion of *in vitro* concentration-response curves for AChE inhibition to *in vivo* dose-response curves for AChE inhibition. However, when developing these PBK models, interethnic differences have not yet been taken into account. Biomonitoring studies have reported OP metabolite levels in maternal urine in China to be higher than those in maternal urine in developed countries (Wang *et al.*, 2012), and interethnic differences in bioactivation and detoxification have already been reported for other compounds than OPs (Ning *et al.*, 2017; Zhang *et al.*, 1990). Hence, it is of importance to include the interethnic differences in kinetics when developing PBK models for CPF in human. To date, several PBK models have been developed for CPF in the Caucasian population (Bouchard *et al.*, 2005; Lu et al., 2009; Mosquin *et al.*, 2009; Timchalk *et al.*, 2002). Knowing that there is no PBK model available that is specifically defined for the Chinese population, the aim of the present study was to investigate, via PBK modeling, the interethnic differences between the Chinese and the Caucasian population in kinetics, biomarkers of exposure, and predicted *in vivo* red blood cell (RBC) AChE inhibition using CPF as the model OP compound.

In present study, CPF was used as model OP because there are available kinetic data for evaluating the performance of the PBK models (Eaton *et al.*, 2008; Griffin *et al.*, 1999; Nolan *et al.*, 1984; Brzak et al., 2000; Timchalk et al., 2002; Bouchard et al., 2005). In humans, CPF will be either detoxified to 3,5,6-trichloro-2-pyridinol (TCPy) and diethyl thiophosphate (DETP) or activated to the corresponding active oxon form chlorpyrifos-oxon (CPO), which inhibits AChE (Figure 1). These 2 pathways have been demonstrated to occur mainly in the liver (Timchalk *et al.*, 2002). Conversion of CPF is catalyzed by cytochromes P450 (CYP450), with CYP2B6 being the most active CYP450 for conversion of CPF into CPO, and CYP2C19 being the most active CYP for conversion of CPF into TCPy and DETP, whereas CYP3A4 is involved in both pathways (Foxenberg *et al.*, 2007; Tang *et al.*, 2001). The detoxification of CPO is catalyzed by A-esterases, with paraoxonase (PON 1) as the major A-esterase involved, resulting in formation of TCPy and diethyl phosphate (DEP) (Figure 1) (Furlong *et al.*, 1989; Timchalk *et al.*, 2002). B-esterase in for example liver, blood, and brain including AChE, butyrylcholinesterase (BChE) and carboxylesterase (CaE) can be bound and inhibited by CPO (Timchalk *et al.*, 2002; Wagner, 1999).

The inhibition of RBC AChE activity has been used as the surrogate endpoint for deriving points of departure (POD) in risk assessment of CPF, such as a benchmark dose (BMD) or a no observed adverse effect level (NOAEL). The rationale for using RBC AChE inhibition as indicator of CPF exposure is based on the fact that RBC AChE is more sensitive and easier to sample compared with AChE in other target organs like brain, spinal cord, and the peripheral nervous system (EPA, 2011). Moreover, it is also known that there is less variation among individuals in the enzyme activity of RBC AChE than plasma BChE (Brock and Brock, 1990; Lefkowitz *et al.*, 2007). Thus, in the present study, the concentration-dependent RBC AChE inhibition by CPO (Eyer *et al.*, 2009) was used as the surrogate endpoint to define the *in vivo* dose-response curves for RBC AChE inhibition in the 2 populations, Chinese and Caucasian, upon CPF exposure.

MATERIALS AND METHODS

Materials

Chemicals. Chlorpyrifos and TCPy were purchased from Sigma-Aldrich (Zwijndrecht, The Netherlands). Chlorpyrifos-oxon was purchased from TRC-Canada (Toronto, Ontario, Canada). Tetraisopropyl pyrophosphoramide (iso-OMPA) and diisopropyl ether (DIPE) were purchased from Sigma-Aldrich (Zwijndrecht, The Netherlands). Magnesium chloride hexahydrate ($MgCl_2$*$6H_2O$), ethylenediaminetetraacetic acid disodium salt dihydrate (EDTA), dipotassium hydrogen phosphate (K_2HPO_4), trifluoroacetic acid (TFA), hydrochloric acid (HCl), perchloric acid ($HClO_4$), dimethylsulfoxide (DMSO), and calcium chloride dihydrate ($CaCl_2$*$2H_2O$) were purchased from VWR International (Amsterdam, The Netherlands). Acetonitrile (ACN, UPLC/MS grade) and methanol (UPLC/MS grade) were purchased from Biosolve (Valkenswaard, The Netherlands). Reduced nicotinamide adenine dinucleotide phosphate (NADPH) was obtained from Sigma-Aldrich (Zwijndrecht, The Netherlands).

Human liver microsomes. Caucasian liver microsomes (pooled from 20 donors, mixed gender) were purchased from Corning (Amsterdam, The Netherlands) and Chinese liver microsomes (pooled from 20 donors, mixed gender) were purchased from Pre-TOX (Wuhan, China).

In Vitro *Incubations to Derive the Kinetic Parameters for the PBK Model*

Human liver microsomal incubations for bioactivation and detoxification of CPF by CYP450 were optimized to be linear in metabolite formation with time and amount of microsomal protein (data not shown). The incubations were carried out in 50 mM phosphate buffer (pH 7.4) containing (final concentrations) 5 mM $MgCl_2$, 1 mM EDTA (A-esterase PON1 inhibitor), 50 μM iso-OMPA (B-esterase inhibitor), 1 mM NADPH (CYP450 cofactor), and CPF (at final concentrations ranging from 5 to 100 μM, added from 100 times concentrated stock solutions in DMSO). Control incubations were performed without the addition of NADPH. After 1 min preincubation, the reaction was initiated by adding 5 μl of either Caucasian or Chinese liver microsomes (final concentration 0.5 mg/ml) and incubated for 15 min (Caucasian) or 30 min (Chinese) in a 37°C water bath. The total volume of the incubation mixtures was 200 μl. The reaction was terminated by the addition of 20 μl ice cold 10% (vol/vol) $HClO_4$.

The PON1-catalyzed metabolism of CPO was measured in the *in vitro* liver microsomal incubations as follows. Preliminary experiments were conducted to define the optimal incubation conditions that are linear in time and with the liver microsomal concentration (data not shown). The kinetic incubations were carried out in 50 mM Tris–HCl (pH 7.4) containing 2 mM $CaCl_2$ (to stimulate the PON1 activity) (Carr *et al.*, 2015), and CPO (at a final concentration range of 25–1500 μM, added from 100 times concentrated stock solutions in DMSO). After 1 min preincubation, the reaction was initiated by adding either 5 μl of Caucasian (final concentration 0.5 mg/ml) or 2.5 μl of Chinese liver

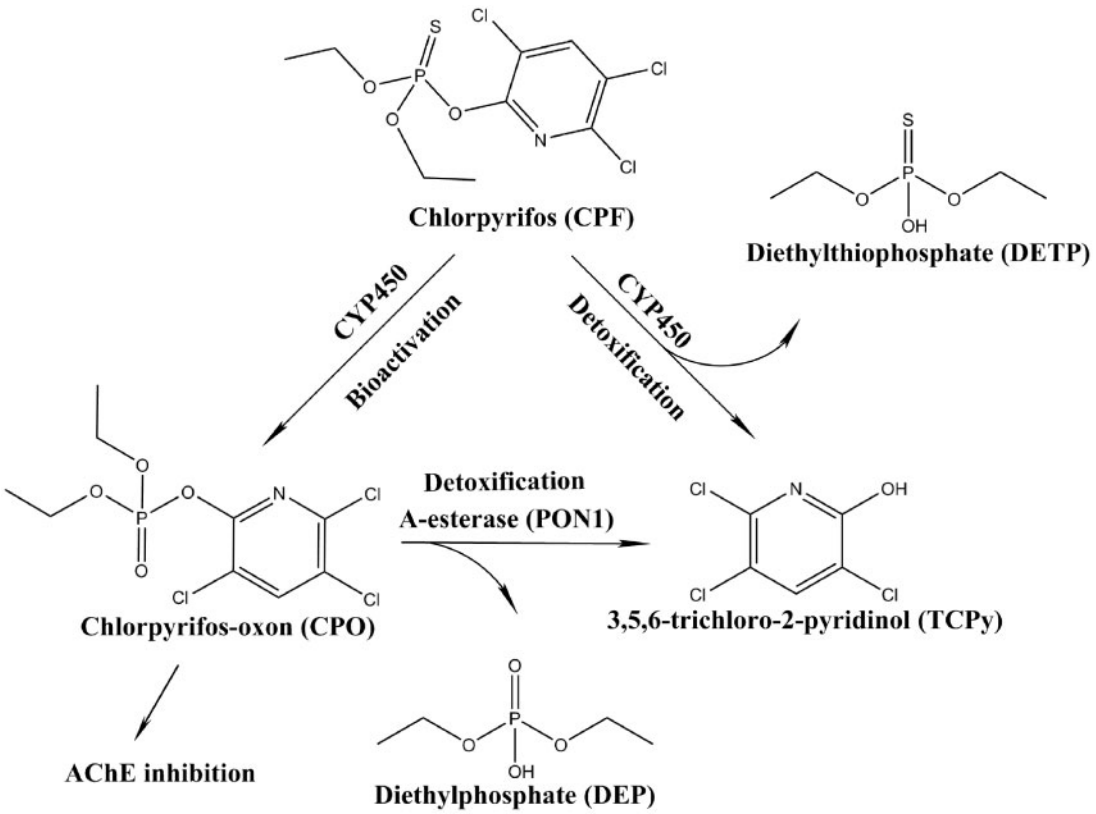

Figure 1. Metabolic pathways for bioactivation and detoxification of CPF (Smith *et al.*, 2011). AChE, acetylcholinesterase; CYP450, cytochrome P450.

microsomes (final concentration 0.25 mg/ml) and incubated for 5 min in a 37°C water bath. Incubations in the absence of microsomes were performed as control. The total volume of the incubation mixtures was 200 µl. The reaction was terminated by the addition of 20 µl ice cold 10% (vol/vol) $HClO_4$ and samples were kept on ice.

Extraction of metabolites was conducted prior to UPLC analysis. To this end, the organic solvent DIPE was added to the ice-cold incubation mixtures. Afterwards, the incubation mixtures were mixed well by vortexing and the upper layer that contained CPF and its metabolites was collected and transferred into a glass tube. The extraction process was conducted 3 times, and the collected DIPE fractions were combined. The extracts were then evaporated to dryness under a stream of nitrogen (N_2). Finally, the extracts containing CPF and its metabolites were redissolved in 100 µl methanol and subsequently used for the UPLC analysis.

It is worth to note that microsomal incubations are well accepted and also validated to define kinetic parameters for metabolism and clearance in PBK modeling (Al-Subeihi et al., 2012; Lu *et al.*, 2009; Mosquin *et al.*, 2009; Ning *et al.*, 2017; Punt *et al.*, 2008, 2009; Timchalk *et al.*, 2002). Furthermore experimental data shown that kinetic data derived from microsomal incubations and hepatocyte incubations are comparable as Di *et al.* (2012) reported that the intrinsic clearance for compounds predominantly mediated by CYP450 obtained from microsomal incubations are comparable with that obtained from hepatocyte incubations.

UPLC Analysis

All redissolved extracts from microsomal incubations of CPF were analyzed by a Waters Acquity UPLC H_class system that consisted of a quaternary solvent manager, a sample manager, and a photodiode array detector, equipped with a Water Acquity UPLC BEH C18 column (1.7 µm, 2.1 × 50 mm) and Waters Xbridge UPLC BEH C18 precolumn (2.5 µM, 2.1 × 5 mm). The temperature of the column was set at 40°C and the auto-sampler at 10°C during the UPLC analysis. The mobile phases used for the analysis consisted of (A) 0.1% TFA in nanopure water and (B) 100% ACN. A gradient elution at a flow rate of 0.6 ml/min was applied for the analysis with the initial condition of 90% A:10% B (vol/vol). The gradient program was set as follows: the starting condition was 90:10 (A:B), changing to 0:100 (A:B) from 0 to 6 min and was maintained for 30 s, and then changed to 100:0 (A:B) in 30 s and was maintained for 1 min. After which, the starting condition were reset from 8 to 8.1 min, and the column was equilibrated at the starting condition of 90:10 (A:B) until 9.5 min. The injection volume for each sample was 3.5 µl. Under these conditions, the retention times of CPF, CPO, and TCPy were 4.8, 3.6, and 2.5 min, respectively. The amount of CPF, CPO, and TCPy was quantified by integrating the peak areas at 299 nm using calibration curves that were prepared using the commercially available standards.

Data Analysis

Kinetic parameters including the apparent maximum velocity (V_{max}; expressed in nmol/min/mg microsomal protein) and the apparent Michaelis–Menten constant (K_m; in µM) for bioactivation of CPF and detoxification of CPF and CPO were obtained by fitting the data using GraphPad Prism 5 software for Windows, version 5.04 (San Diego, California) to the standard Michaelis–Menten equation:

$$V = V_{max} * [S]/(K_m + [S])$$

in which the S represents the concentration of substrate in μM.

Physiologically based kinetic (PBK) model

Model structure. Figure 2 illustrates the structure of the CPF PBK model for both the Chinese and Caucasian population. The model was developed based on the model reported by Timchalk *et al.* (2002) with some modifications. The model contained separated compartments for the gastrointestinal tract (GI-tract), blood, fat, liver, slowly perfused tissue (muscle, skin, and bone), and rapidly perfused tissue. The bioavailability of CPF upon oral exposure was included by taking the fractional absorption (fa) into account. This fa was found to vary across human volunteer studies, amounting to 0.22 (22% of the oral dose being absorbed) (Bouchard *et al.*, 2005), 0.224 (Timchalk *et al.*, 2002), 0.70 (Nolan *et al.*, 1984), and 0.93 (Bouchard *et al.*, 2005; Griffin *et al.*, 1999), respectively, in part depending on the form of CPF administration (Timchalk *et al.*, 2002). When modeling the data, the fa values reported by Timchalk *et al.* (2002; fa = 0.224) and Nolan *et al.* (1984; fa = 0.70) were used, and the mean of those 2 fa values, which is 0.462, was also included. First-order kinetics was used to describe the absorption of CPF by the GI tract with an absorption rate constant of 0.46/h (Bouchard *et al.*, 2005). The absorbed CPF was assumed to be transferred to the liver compartment without intestinal biotransformation based on the fact that intestinal CPF biotransformation was reported to be limited compared with that in the liver (Leoni *et al.*, 2012). Furthermore, CYP450-mediated conversion of CPF was assumed to occur only in the liver because liver is known to be the main organ for CYP450-mediated biotransformation of CPF (Leoni *et al.*, 2012). This metabolism resulted in formation of TCPy and DETP, and of CPO (Figure 1). Based on a preliminary experiment (data not shown), the conversion of CPF by A-esterase (PON1) appeared to be negligible compared with the CYP450-catalyzed reaction and thus was not included in the model. The PBK model also contained a sub-model describing the kinetics of CPO. The formation of CPO from CYP450-mediated conversion of CPF in the liver compartment provided the input of CPO for this CPO sub-model, in which CPO was predicted to be further converted to TCPy and DEP in both the liver and blood compartment mediated by A-esterase (PON1). The cumulative urinary excretion of TCPy and of the dialkylphosphate (defined as the sum of DEP and DETP) was described by applying first-order rate equations with the first-order rate constants amounting to 0.026/h and 0.199/h, respectively (Bouchard *et al.*, 2005). The Rosenbrock's algorithm for stiff systems was used to code the differential equations and the mass balance in Berkeley Madonna software (Macey and Oster, UC Berkeley, California). The PBK model differential equations are provided in the Supplementary Data I.

Model parameters. The physiological parameters for both the Chinese and Caucasian population were collected from the literature (Brown *et al.*, 1997; NHFPC, 2007a,b, 2014) and are presented in Table 1. The physico-chemical parameters (tissue:blood partition coefficients) for CPF and CPO, also presented in Table 1, were determined based on clog*P* using ChemDraw Professional 16.0 software (CambrigeSoft), using the method described by DeJongh *et al.* (1997). The kinetic parameters for conversion of CPF and CPO in the liver were determined in the present study and are summarized in Table 2 and presented in some more details in the Results section. For PON1-mediated detoxification of CPO to TCPy in blood, the V_{max} expressed in μmol/h/kg $bw^{0.75}$ for the Caucasian population, obtained from plasma enzymatic incubations (Furlong *et al.*, 1989; Mosquin *et al.*, 2009), was multiplied by the $bw^{0.75}$ of the Chinese and Caucasian, respectively, to obtain the corresponding value for both populations expressed in μmol/h. A hepatic microsomal protein scaling factor of 32 mg microsomal protein/g liver (Al-Malahmeh et al., 2017; Barter *et al.*, 2007) was applied to scale the apparent V_{maxc} from μmol/min/mg microsomal protein to the V_{max} expressed in μmol/min/g liver. Furthermore, the V_{max} was expressed in μmol/h/kg liver.

Model validation. To validate the model, the PBK model-predicted blood concentration of TCPy and the cumulative urinary amount of TCPy were compared with reported *in vivo* data (Bouchard *et al.*, 2005; Nolan *et al.*, 1984; Timchalk *et al.*, 2002).

Sensitivity analysis. The impact of each parameter on the model output (in this study especially the blood concentrations of CPO) was estimated by performing a sensitivity analysis. Normalized sensitivity coefficient (SC) was determined based on the following equation:

$$SC = (C' - C)/(P' - P) * (P/C)$$

in which *P* represents the parameter value in the PBK model and *P′* represents the parameter value with a 5% increase (Evans and Andersen, 2000). Similarly, *C* is the output of the model with the original model parameter value and *C′* the model output with 5% increase in the model parameter value. Only parameters with SC > 0.15 (absolute value) are presented in the current manuscript (Figure 7).

Reverse Dosimetry

Derivation of a concentration-response curve for RBC AChE inhibition. In the present study, the concentration-response curve for CPO-mediated RBC AChE inhibition reported by Eyer *et al.* (2009) was used, who quantified the level of AChE inhibition upon incubating plasma samples from CPF-poisoned patients (with quantified level of CPO) with hemolysate from an unexposed donor to determine the level of AChE inhibition (Eyer *et al.*, 2009).

Conversion of concentration-response curves to in vivo *dose-response curves for RBC AChE inhibition*. The concentration-response curve for RBC AChE inhibition by CPO in human was obtained from Eyer *et al.* (2009), and used as input to quantify the maximum blood concentration (C_{max}) of CPO in the PBK models for calculating the corresponding dose levels. By performing this calculation for all the concentrations, the concentration-response curve for RBC AChE inhibition was converted to an *in vivo* dose-response curve for CPF-induced RBC AChE inhibition. Given that the concentrations in the concentration-response curve represented the total concentration of CPO (Eyer *et al.*, 2009; Heilmair *et al.*, 2008), the concentration values of the concentration-response curve could be directly used as input in the PBK models. By performing the reverse dosimetry using the PBK model for the Caucasian and Chinese population, *in vivo* dose-response curves for both ethnic groups were predicted.

Validation of predicted dose-response curves for RBC AChE inhibition. To validate the performance of the PBK model-facilitated reverse dosimetry approach, the predicted dose-response curve for RBC AChE inhibition upon exposure to CPF for the Caucasian population was compared with available *in vivo* data (EPA, 1999; Timchalk *et al.*, 2002). Evaluation of the Chinese PBK model was

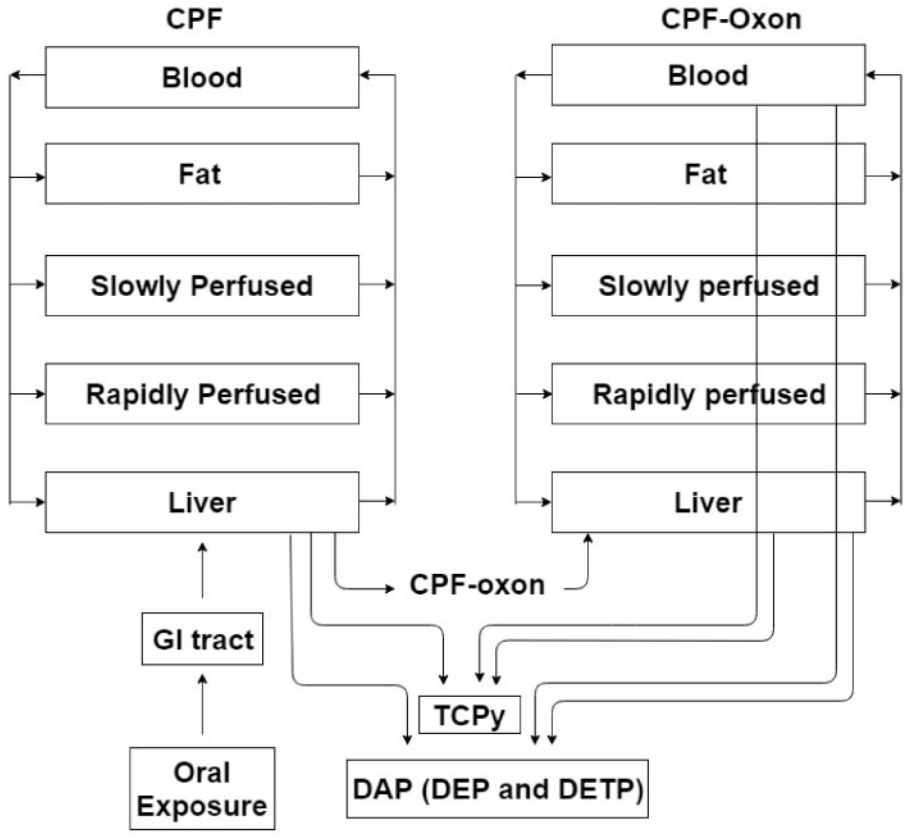

Figure 2. Schematic diagram of the PBK model for CPF (Timchalk *et al.*, 2002) in the Chinese and Caucasian population, consisting of 2 models including one for CPF (left) and one submodel for CPO (right). GI tract, gastrointestinal tract.

based on the evaluation of the Caucasian model combined with the fact that both models were defined in the same way.

Derivation of BMD and BMDL

The predicted dose-response curves were used to derive PODs for CPF risk assessment for these 2 populations. Because the data were not suitable for BMD modeling, the effective dose $(ED)_{10/20}$ value for CPF in the Chinese and Caucasian was defined at 10% or 20% inhibition of RBC AChE. Subsequently, taking into account that a BMDL should not be more than a factor 3 below a BMD value to provide an adequate POD, the obtained $ED_{10/20}$ values were divided by 3 to obtain POD values that could be compared with the PODs reported by The European Food Safety Authority (EFSA, 2014) and EPA (BfR, 2012; Fan, 2014; Koshlukova and Reed, 2014).

RESULTS

In Vitro Metabolism of CPF and CPO

The CYP450-mediated conversion of CPF to CPO and TCPy was measured in incubations with both Chinese and Caucasian liver microsomes. No metabolites were detected in control incubation performed in the absence of NADPH. The PON1-mediated conversion of CPO to TCPy was detected in both population, Chinese and Caucasian, of liver microsomal incubations, whereas in the absence of liver microsomes, some TCPy was detected, mainly ascribed to an impurity in the CPO starting material (data not shown). Thus, results obtained in the presence of liver microsomes were corrected for the TCPy detected in control incubation without microsomes.

The concentration-dependent increase in metabolite formation following incubations of CPF and CPO with both Chinese and Caucasian liver microsomes is depicted in Figure 3. The kinetic parameters K_m and V_{max} derived from these results as well as the catalytic efficiency, calculated as V_{max}/K_m, are presented in Table 2.

The results presented in Figure 3 and Table 2 indicate that there is a difference in the catalytic efficiency for conversion of CPF and CPO by the Chinese and Caucasian population. The catalytic efficiency for bioactivation of CPF to CPO was around 4.5-fold less efficient in incubations with Chinese than with Caucasian liver microsomes, due to a 2.8-fold lower V_{max} and a 1.6-fold higher K_m (Table 2). However, Chinese liver microsomes were only 2 times less efficient than Caucasian liver microsomes in detoxification of CPF to TCPy. In addition, Chinese liver microsomes appeared to be 2.8 times more efficient in the detoxification of CPO into TCPy than Caucasian liver microsomes.

PBK Model Validation

The developed PBK model of CPF was evaluated against *in vivo* data from human volunteer studies in the Caucasian population (Bouchard *et al.*, 2005; Nolan *et al.*, 1984; Timchalk *et al.*, 2002). The model was first evaluated using the data from Nolan *et al.* (1984). Figure 4A presents the model-predicted and reported amount of TCPy eliminated in urine using an fa of 0.70, as reported by Nolan *et al.* (1984). In addition, Figure 4B compares the model-predicted blood concentration of TCPy and the reported data. These results indicate that the predictions made by the newly developed PBK model match the reported data

Table 1. Summary of Physiological and Physicochemical Parameters for the PBK Models for CPF and Its Metabolites in the Caucasian and Chinese population (Brown *et al.*, 1997; DeJongh *et al.*, 1997; NHFPC, 2007a,b, 2014)

Model parameters	Caucasian	Chinese
Physiological parameters		
Body weight (kg)	70	58.5
Percentage of body weight		
Liver	2.6	2.3
Fat	21.4	18.4
Rapidly perfused	5.4	6.9
Slowly perfused	58	57.3
Blood	7.9	7.9
Flow(l/h)		
Cardiac output	347.9	327
Percentage of cardiac output		
Liver	22.7	26.3
Fat	5.2	6.8
Rapidly perfused	43	42.4
Slowly perfused	29.1	24.5
Tissue: blood partition coefficients for CPF		
Liver	8.1	8.1
Fat	142	142
Rapidly perfused	8.1	8.1
Slowly perfused	5.2	5.2
Tissue: blood partition coefficients for CPO		
Liver	4.9	4.9
Fat	119.3	119.3
Rapidly perfused	4.9	4.9
Slowly perfused	3.3	3.3

The kinetic parameters for the PBK models are presented in Table 2.
Abbreviations: PBK, physiologically based kinetic; CPF, chlorpyrifos; CPO, chlorpyrifos-oxon.

quite well, and in a manner comparable with the model reported before by Lu et al. (2009). However, a best fit between model-predicted TCPy blood concentration and *in vivo* data could be achieved (Figure 4) by increasing the volume of distribution for TCPy (Vd) from 5.53 l (setting the Vd equal to the average human blood volume (VB; Brown *et al.*, 1997)) to 15 l. This 15 l was obtained by fitting the model to *in vivo* data (Nolan *et al.*, 1984) similar as done by others (Mosquin *et al.*, 2009; Timchalk *et al.* 2002). Together these data illustrate how the currently developed PBK model can adequately match the reported *in vivo* data.

In a next step, a comparison was made to the data reported by Timchalk *et al.* (2002) and Lu et al. (2009) to further evaluate the developed-PBK model (Figure 5). The application of fa = 0.224, as reported by this literature, was set in the defined PBK model for the Caucasian population, resulting in a good match between predicted and experimental human *in vivo* data (Lu et al., 2009; Timchalk *et al.*, 2002). Also, the model adequately predicted the blood concentration of TCPy with 3-fold deviation from the data reported by Timchalk *et al.* (2002). Using a Vd of 15 l, fitting this model parameter Vd to the *in vivo* data as done by Timchalk *et al.* (2002) and Mosquin *et al.* (2009), a better fit was even obtained (see Figure 5).

Finally, the performance of the model was evaluated based on the experimental data originally from Brzak (2000) but reported by Bouchard *et al.* (2005) using an fa of 0.22 (Bouchard *et al.*, 2005) (Figure 6). The results reveal that also for this data set, the newly developed PBK model closely predicted both the cumulative amount of TCPy eliminated in urine and the blood concentration of TCPy at all 3 dose levels tested. The predicted TCPy concentration in blood were around 3-fold higher than what was actually observed *in vivo*. As observed from the other data sets, these matches could be further improved by changing the value of Vd to 15 l, based on fitting this model parameter to the *in vivo* data as done by others (Mosquin *et al.*, 2009; Timchalk *et al.* 2002) (see Figure 6).

Although some underestimation is still observed at later time points after reaching the maximum TCPy blood concentration when comparing our prediction with the *in vivo* data from Timchalk *et al.* (2002) as well as with the data from Brzak (2000) after changing the Vd to 15 l. These inter-study differences are mainly caused by the TCPy elimination rate constant (Ke) that we used because the value of Ke (0.026/h) that we used in our model was obtained from Nolan *et al.* (1984) but not obtained by fitting model to data from Nolan *et al.* (1984) as what others did (Ke = 0.017/h in Timchalk *et al.*, 2002 and Ke = 0.03820/h in Mosquin *et al.*, 2009). Thus, these fits can be improved even further if we fit Ke (0.019/h) in the model to *in vivo* data Nolan *et al.* (1984) in line with what others did (Mosquin *et al.*, 2009; Timchalk *et al.*, 2002) (Supplementary Data V and VI).

In our later prediction, we assumed the Vd for TCPy to be equal to human blood volume (5.53 l, Brown *et al.*, 1997), which has physiological meaning, and Ke equal to 0.026/h. Nevertheless, a better match between the model prediction and *in vivo* data for the blood concentration of TCPy could be obtained when the Vd value was increased to 15 l. The match between the model prediction and *in vivo* data sets from Timchalk *et al.* (2002) and Brzak (2000) can be further improved by changing Ke to 0.019/h (both of these 2 parameters were obtained by fitting the model to the *in vivo* data Nolan *et al.* (1984) as done by others (Mosquin *et al.*, 2009; Timchalk *et al.* 2002). However, it is important to note as well that changing the value of Vd and value of Ke did not affect the prediction of the CPO concentration in blood, and thus also did not affect the resulting prediction for AChE inhibition (data not shown).

Due to a lack of kinetic data for Chinese subjects, evaluation of the performance of the PBK model for CPF in the Chinese population was based on this validation of the Caucasian model.

Sensitivity Analysis

A sensitivity analysis was performed at a dose of 0.5 mg CPF/kg bw and of 180 mg CPF/kg bw (Timchalk *et al.*, 2002) to determine the impact of each parameter on the predicted blood C_{max} of CPO in the Chinese and the Caucasian PBK models. Figure 7 presents the values for which the SC was higher than 0.15 (absolute value). Comparing the results of the sensitivity analysis for the Chinese PBK model with that of the Caucasian PBK model, a similar result was obtained at both dose levels. For both the Chinese and the Caucasian model, the prediction of the C_{max} of CPO appeared to be mainly affected by the kinetic parameters for hepatic CPO formation as well as the kinetic parameters for hepatic detoxification of CPO to TCPy, although the fa also significantly affected the C_{max} of CPO (Figure 7A). In addition, the C_{max} of CPO was also influenced by blood flow from various compartments (liver to blood, rapidly perfused tissue to blood and slowly perfused tissue to blood). For physiological parameters, volume of liver was found to have the largest impact in both the Caucasian and the Chinese model. At the higher dose of 180 mg/kg bw, similar results were obtained except for a somewhat lower impact of the kinetic parameters for conversion of CPF to TCPy.

Table 2. Summary of Kinetic Parameters (K_m, unscaled/scaled V_{max}) and Catalytic Efficiency (V_{max}/K_m), for Metabolism of CPF and CPO (Barter *et al.*, 2007; Brown *et al.*, 1997; Furlong *et al.*, 1989; Mosquin *et al.*, 2009; NHFPC, 2007a)

Ethnic Pathway	Caucasian	Chinese
CPF to CPO (Liver)		
K_{m1} (μM)	28.59 ± 6.60	44.91 ± 34.90
In vitro V_{max1c} (nmol / min / mg microsomal protein)	0.156 ± 0.014	0.055 ± 0.019
In vitro Catalytic efficiency (V_{max1c} / K_{m1}) [ab]	5.5	1.2
In vivo scaled V_{max1} (μmol / h / kg liver) [c]	300 ± 27	106 ± 36
In vivo scaled Catalytic efficiency (V_{max1} / K_{m1}) [d]	10.49	2.36
CPF to TCPy (Liver)		
K_{m2} (μM)	4.33 ± 0.56	3.16 ± 0.745
In vitro V_{max2c} (nmol / min / mg microsomal protein)	0.234 ± 0.006	0.093 ± 0.004
In vitro Catalytic efficiency (V_{max2c} / K_{m2}) [ab]	54.0	29.4
In vivo scaled V_{max2} (μmol / h / kg liver) [c]	449 ± 12	179 ± 8
In vivo scaled Catalytic efficiency (V_{max2} / K_{m2}) [d]	103.7	56.6
CPO to TCPy (Liver)		
K_{m3} (μM)	627.90 ± 165.00	660.70 ± 167.00
In vitro V_{max3c} (nmol / min / mg microsomal protein)	37.98 ± 4.33	111.90 ± 12.51
In vitro Catalytic efficiency (V_{max3c} / K_{m3}) [ab]	60.5	169.4
In vivo scaled V_{max3} (μmol / h / kg liver) [c]	72922 ± 8314	214848 ± 24019
In vivo scaled Catalytic efficiency (V_{max3} / K_{m3}) [d]	116.1	325.2
CPO to TCPy (Blood)		
K_{m4} (μM)	75	75
V_{max4c} (μmol / h / $kg^{0.75}$ body weight)	4.4	4.4
Catalytic efficiency (V_{max4c} / K_{m4}) [e]	0.05867	0.05867
V_{max4} (μmol / h) [f]	106.48	93.28
Catalytic efficiency (V_{max4} / K_{m4}) [g]	1.41973	1.24373

[a] μl / min / mg microsomal protein
[b] V_{maxc} /K_m *1000
[c] $V_{max} = V_{maxc}$ / 1000* 60 * 32 *1000 , where the 32 is the scaling factor to scale the V_{maxc} from nmol/min/mg microsomal protein to nmol/min/g liver, 1000 is for changing unit from nmol to μmol, the 60 is for changing the unit from min to h and 1000 is for changing the unit from g to kg (liver).
[d] l / h / kg liver
[e] l / h / $kg^{0.75}$ body weight
[f] V_{max4} (μmol/h/kg liver) = V_{max4c} * body weight $^{0.75}$, the body weight could be either the Caucasian body weight (70 kg) or the Chinese body weight (58.5kg)
[g] l / h

PBK Model Predictions

Dose-dependent blood concentrations of CPO. After PBK model validation, the defined models were used to quantify the dose-dependent blood C_{max} of CPO in both populations using not only fa = 0.224 (Figure 8A) but also fa = 0.462 and fa = 0.70 (presented in Supplementary Data II) in order to take into account the different values reported in the literature of CPF bioavailability. Comparison of the blood C_{max} of CPO at increasing dose levels in the Chinese and the Caucasian population, reveals a 5- to 8-fold difference in the C_{max} values between the Caucasian and the Chinese population, with the C_{max} values for the Caucasian population being higher (Figure 8A). This difference originates from the less efficient bioactivation of CFP to CPO and the more efficient detoxification of CPO in the Chinese as compared with the Caucasian population, which already noted above. Clearly, the PBK model integrates the kinetic data for the individual reactions enabling prediction of the overall effect on the C_{max} for CPO.

Time- and dose-dependent cumulative urinary excretion of TCPy. The defined PBK models were also used to predict the time- and dose-dependent cumulative urinary excretion of TCPy in both ethnic groups, in order to capture the possible ethnic differences when using urinary TCPy as a biomarker for exposure assessment. The time-dependent cumulative excretion was predicted to increase especially over the first 72 h. The time-dependent urinary TCPy excretion at a dose level of 0.5 mg/kg was predicted to be 1- to 2-fold higher in the Caucasian than in the Chinese population, and a similar pattern was observed at a higher CPF dose of 180 mg/kg bw (data for fa = 0.224 presented in Figs. 8B and 8C, data for fa = 0.46 and fa = 0.70 presented in Supplementary Data II). The CPF dose-dependent urinary excretion of TCPy (data for fa = 0.224 are presented in Figure 8D, data for fa = 0.46 and fa = 0.70 are presented in Supplementary Data II) reveals a difference in urinary TCPy levels at similar dose levels at both 24 and 72 h, with the levels in Caucasians being higher than those in Chinese (Figure 8D). The curves also indicate that to reach a similar urinary TCPy elimination as in the Caucasian, the corresponding dose level of CPF exposure may vary from 1.3- to 5-fold higher in the Chinese, depending on the duration for urinary collection, the CPF dose and the fa (Figure 8D).

Interethnic differences in CPF dose-dependent inhibition of AChE. In a next step, the CPO concentration-dependent AChE inhibition curve reported by Eyer *et al.* (2009) was converted into CPF dose-dependent curves for AChE inhibition in the Caucasian and Chinese population using PBK model-facilitated reverse dosimetry to calculate the dose levels required to generate the respective CPO C_{max} values. Figure 9 presents the predicted *in vivo* dose-response curves for CPF-mediated AChE inhibition in the Caucasian and Chinese population using the 3 different values

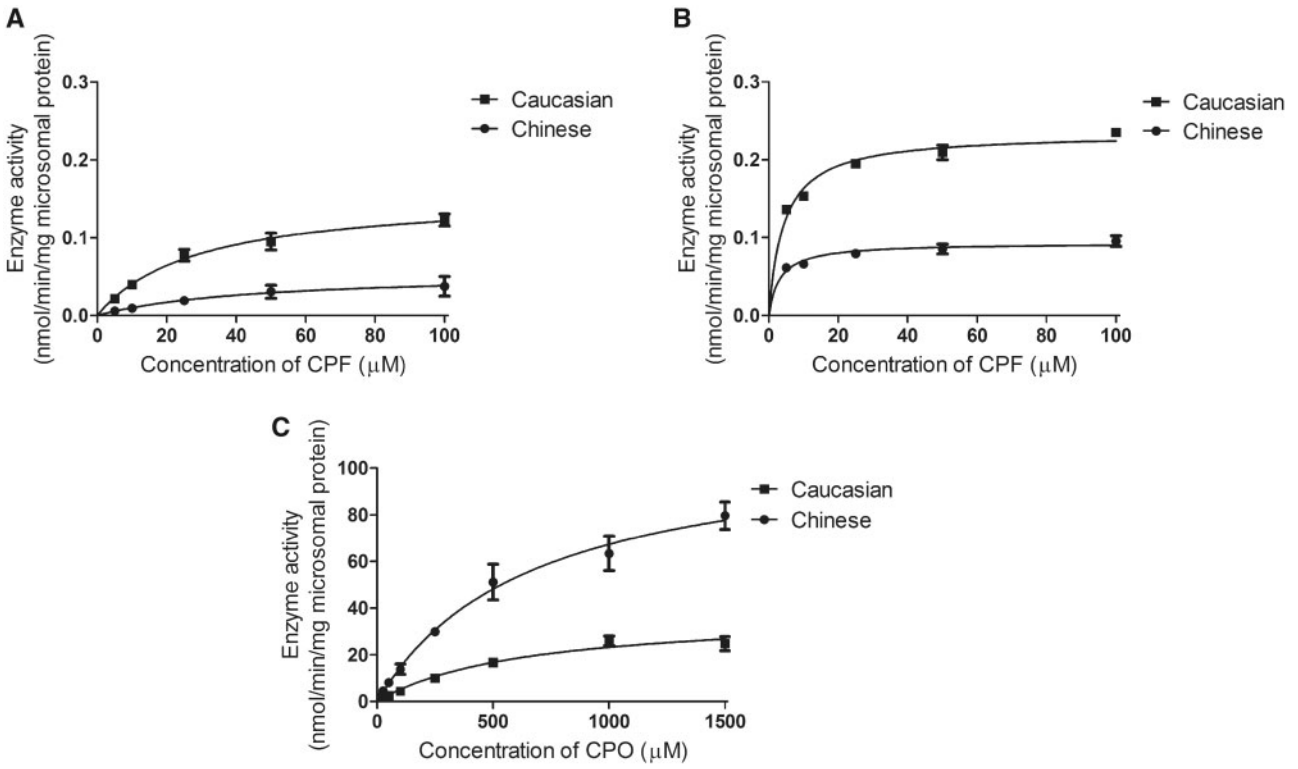

Figure 3. Comparison of the concentration-dependent rate of conversion of (A) CPF to CPO, (B) CPF to TCPy, and (C) CPO to TCPy, in incubations with Caucasian (solid squares) and Chinese (solid circles) liver microsomes. Results represent data from 3 independent experiments and are presented as mean ± SEM.

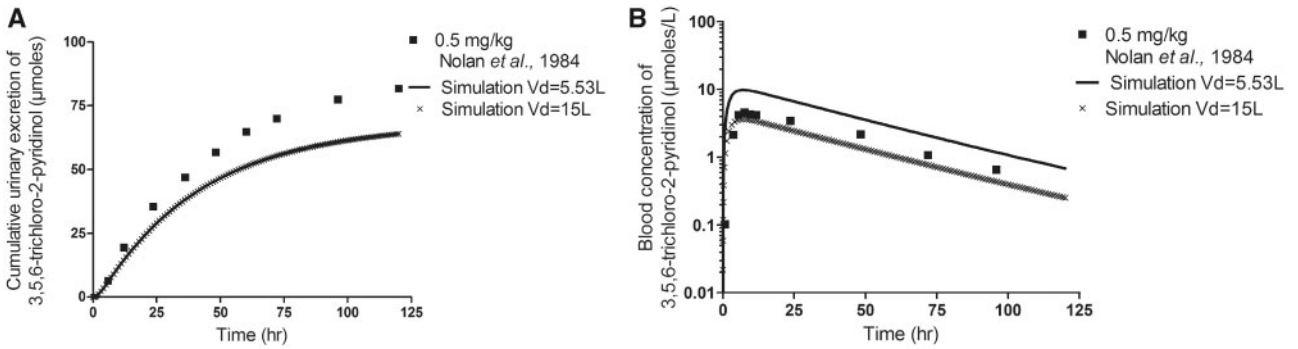

Figure 4. Comparison of PBK model-predicted and experimentally determined time-dependent (A) cumulative urinary excretion of TCPy and (B) blood concentrations of TCPy in Caucasian volunteers upon oral administration of 0.5 mg CPF/kg bw (Nolan *et al.*, 1984). The simulations were performed using an fa equal to 0.70, and either Vd = 5.53 l (solid line) or Vd = 15 l (cross line), whereas the squares represent the values from the human volunteer study (Nolan *et al.*, 1984).

for fa. Figure 9 also presents available experimental data for *in vivo* CPF dose-dependent inhibition of AChE (solid circle/unfilled square). These results reveal that predicted *in vivo* dose-response curves for RBC AChE inhibition in the Caucasian population were comparable with reported *in vivo* data (EPA, 1999; Timchalk *et al.*, 2002), with the best fit obtained for an fa of 0.462. Data for Chinese subjects for further evaluation of the predicted dose-response curves were not available.

From the results presented in Figure 9, it follows that in the Chinese population similar AChE inhibition is reached at a 4- to 7-fold higher dose than in the Caucasian population. This indicates that the Chinese population is less sensitive to CPF-mediated AChE inhibition and CPF-related adverse effects than the Caucasian population. Analysis of the differences in the kinetics reveals that this is mainly due to an approximately 4.5-fold less efficient bioactivation of CPF to CPO combined with a 2.8-fold more efficient detoxification of CPO (Table 2).

Defining a point of departure for risk assessment. In a final step, the predicted dose-response curves were used to derive a POD for risk and safety assessment of CPF. To this end, the ED resulting from 10% or 20% inhibition of RBC AChE was derived from the dose-response curves for both the Caucasian and Chinese population, and was divided by 3 to obtain PODs that would be comparable with BMDL or NOAEL values used as PODs in previous risk assessments (BfR, 2012; EFSA, 2014; Fan, 2014; Koshlukova and Reed, 2014). A 20% inhibition of AChE has been defined before by EFSA to obtain a suitable POD to define the acute reference dose for CPF (EFSA, 2014) whereas EPA in its risk assessment of CPF established a $BMDL_{10}$ resulting in

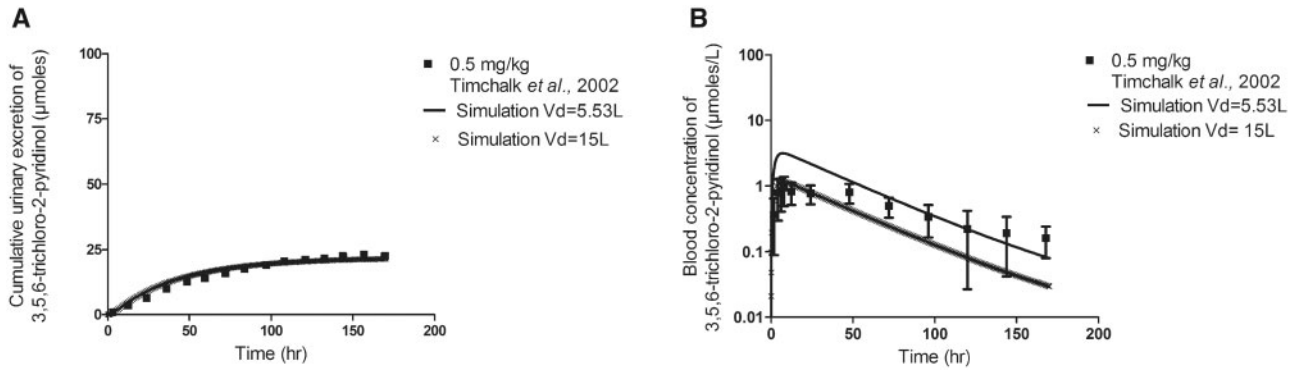

Figure 5. Comparison of PBK model-predicted and experimentally determined time-dependent (A) cumulative urinary excretion of TCPy (Lu et al., 2009; Timchalk *et al.*, 2002) and (B) blood concentrations of TCPy in Caucasian volunteers upon oral administration of 0.5 mg CPF/kg bw (Timchalk *et al.*, 2002). The simulations were performed using fa = 0.224, and either Vd = 5.53 l (solid line) or Vd = 15 l (cross line), whereas the squares symbols represent the values from the human volunteer study (Timchalk *et al.*, 2002).

10% RBC AChE inhibition as POD (BfR, 2012; Fan, 2014; Koshlukova and Reed, 2014). More recently, EPA indicated that 10% RBC AChE inhibition may not be adequately protective for human health because several studies suggested that adverse effects could occur even at lower levels of RBC AChE inhibition (EPA, 2016).

In Figure 10, the obtained PODs for CPF are compared with the POD established by EFSA based on 20% RBC AChE inhibition in pups (EFSA, 2014) and the $BMDL_{10}$ defined by EPA (BfR, 2012; Fan, 2014; Koshlukova and Reed, 2014). The values are summarized in Supplementary Data III to also specify the influence of the fa on the values obtained. The comparison reveals that the predicted PODs derived in the present study using the PBK model–based reverse dosimetry are comparable with the PODs defined by EFSA and EPA. The reported reference value of 0.5 mg/kg bw reported by EFSA (2014) is (depending on the fa value) 0.6 to 1.8-fold higher compared with the predicted $ED_{20}/3$ value for Caucasians and is 0.1 to 0.3-fold higher compared with the predicted $ED_{20}/3$ value for the Chinese population. When compared with the EPA reported $BMDL_{10}$ of 0.36 mg/kg bw (BfR, 2012; Fan, 2014; Koshlukova and Reed, 2014), the predicted $ED_{10}/3$ values for the Caucasian and the Chinese population are 1.3 to 4.3-fold lower and 0.2 to 0.8-fold higher, respectively, indicating an interethnic variation, with values for the Chinese population being approximately 5- to 6-fold higher than those for the Caucasians, reflecting the lower sensitivity of the Chinese population.

DISCUSSION

The aim of the present study was to investigate the interethnic differences in kinetics, biomarker formation, and *in vivo* RBC AChE inhibition for CPF in the Chinese and the Caucasian population. To this end, CPF PBK models were developed for the Chinese and the Caucasian population and subsequently used for the prediction of time- and dose-dependent interethnic differences in kinetics and biomarker formation as well as for reverse dosimetry to translate CPO concentration-dependent data on inhibition of RBC AChE to *in vivo* dose-response curves for CPF-induced inhibition of RBC AChE.

The results obtained revealed a marked interethnic difference in toxicokinetics of CPF, with CYP450-mediated bioactivation to CPO being lower in Chinese, but PON1-mediated detoxification of CPO being higher in Chinese, resulting in higher predicted blood C_{max} values for the toxic metabolite CPO in the Caucasian than in the Chinese population at similar dose levels (Figure 8A). This interethnic difference in toxicokinetics of CPF may be related to differences between the ethnic groups in the frequency of different alleles of the relevant CYP2B6, CYP2C19, CYP3A4, and PON1 enzymes. For example, lower frequencies for 2 CYP2B6 single-nucleotide polymorphisms (SNPs) have been observed in the Chinese population (Guan *et al.*, 2006), SNPs that were shown to result in a relatively higher catalytic efficiency for 7-ethoxy-4-trifluoromethylcoumarin O-deethylation (substrate of CYP2B6) compared with wild type (Guan *et al.*, 2006; Jinno *et al.*, 2003), suggesting that the Chinese population might be less efficient in CYP2B6-catalyzed CPO formation than the Caucasian. Besides, it has been documented that the catalytic efficiency for hydroxylation of the CYP2B6 substrate bupropion by Chinese microsomes was 1.8-fold lower than that for Caucasian microsomes (Yang et al., 2012). Moreover, Barter *et al.* (2013) reported that the hepatic abundance of CYP2C19 is only 8 pmol/mg in Chinese but 14 pmol/mg in Caucasian, and the frequency of CYP2C19 poor metabolizers is 13% in Chinese but only 2.4% in Caucasian. In addition, it has been reported that PON1R192 hydrolyses CPO faster than PON1Q192 (Ali and Chia, 2008; Eyer *et al.*, 2009; Mutch *et al.*, 2007), so that a higher efficiency of CPO hydrolysis in the Chinese population could be due to a relatively higher frequency of the RR genotype in the Chinese. To our knowledge, no comparison of genotype frequency of hepatic PON1 among these 2 races has been reported, but a study by Ali and Chia (2008) showed that Chinese have a higher RR genotype frequency (33%) of plasma PON1 than Caucasians (8.7%). Because plasma PON1 activity may result from release of the enzyme from the liver (Ali and Chia, 2008), similar differences might be expected in liver PON1 activity.

Evaluation of the developed PBK model against literature data available on cumulative urinary elimination of TCPy and blood C_{max} of TCPy (Bouchard *et al.*, 2005; Nolan *et al.*, 1984; Timchalk *et al.*, 2002), indicated that the model was highly sensitive to the fa. However, when taking the fa reported in the respective studies into account revealed that the defined PBK model was able to adequately predict the kinetics of CPF in the human body. In subsequent steps the PBK models were used to evaluate interethnic variation in biomarker formation and toxicity of CPF.

The prediction of cumulative urinary TCPy elimination, which often used as a biomarker for CPF exposure, revealed an

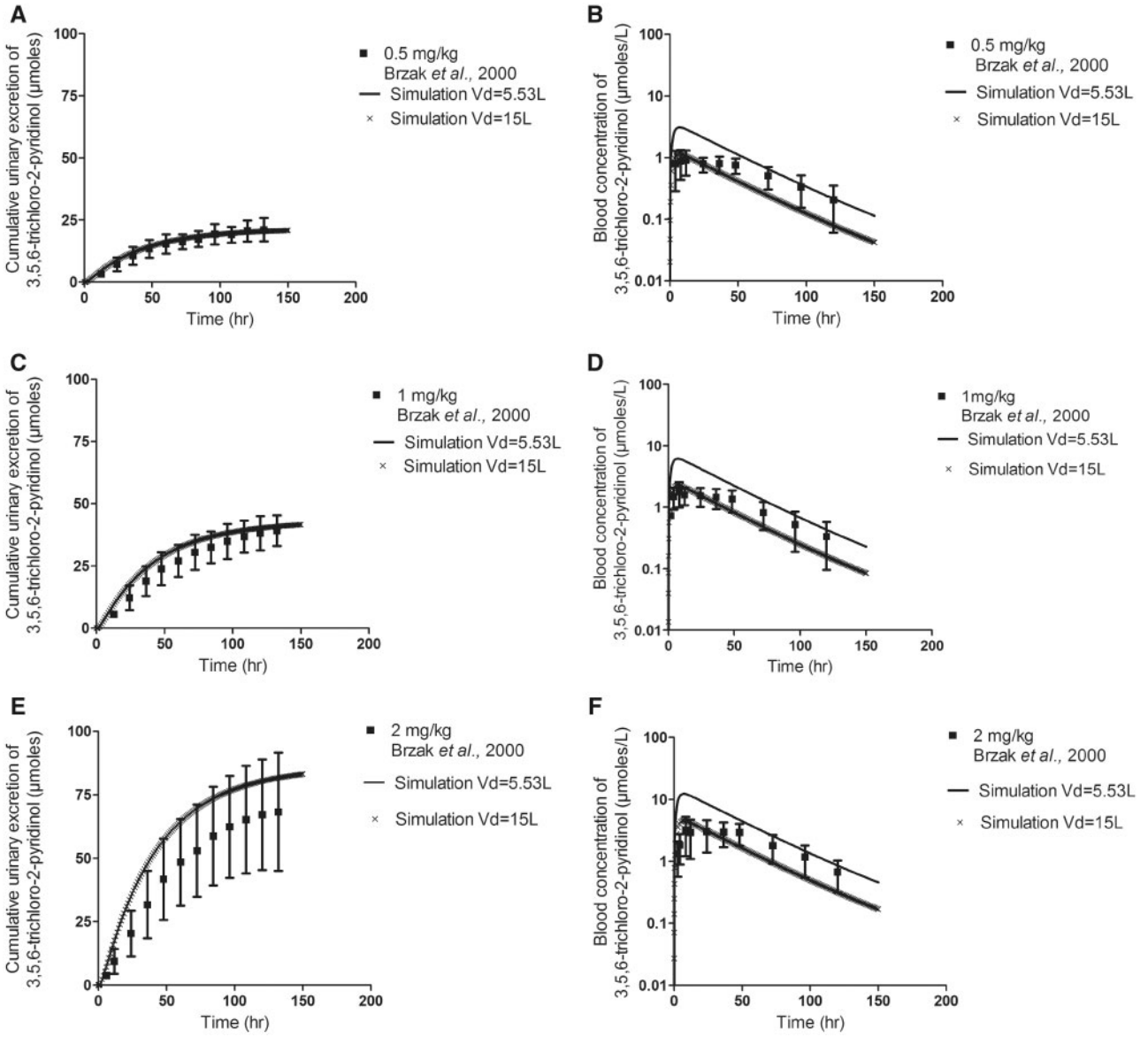

Figure 6. Comparison of PBK model-predicted and experimentally determined time-dependent cumulative urinary excretion of TCPy at an oral dose of (A) 0.5 mg CPF/kg bw, (C) 1.0 mg CPF/kg bw, and (E) 2 mg CPF/kg bw, and of PBK model predicted and experimentally determined blood concentration of TCPy at an oral dose of (B) 0.5 mg CPF/kg bw, (D) 1 mg CPF/kg bw, and (F) 2 mg CPF/kg bw. The simulations were performed using fa = 0.22, and either Vd = 5.53 l (solid line) or Vd = 15 l (cross line), whereas the squares represent the valued took from Bouchard *et al.* (2005) which originally from Brzak (2000).

around 2-fold lower cumulative TCPy elimination in the Chinese than the Caucasian when they were exposed to the same CPF dose level (Figure 8D). In other words, to reach a similar urinary TCPy elimination as the Caucasian, the corresponding dose level of CPF exposure should be 1.3- to 5-fold higher in the Chinese (Figure 8D). These results imply that when using urinary TCPy elimination as a biomarker for the CPF exposure of the Chinese population, dose levels will be relatively underestimated for the Chinese population if these interethnic differences are not taken into account.

The consequences of interethnic differences in CPF kinetics for its potential toxicity for Chinese and Caucasians were also investigated using PBK modeling-facilitated reverse dosimetry. To that end, the CPO concentration-dependent curve for RBC AChE inhibition (Eyer *et al.*, 2009) was translated to *in vivo* dose-response curves for CPF-mediated RBC AChE inhibition for both ethnic groups. The data thus obtained for the Caucasian matched with the available *in vivo* human data available for this ethnic group (Figure 9). This further validates the developed-CPF PBK models and also provides support for the *in vitro*-PBK model-facilitated reverse dosimetry approach to obtain *in vivo* dose-response curves suitable for defining PODs for risk assessment. In line with the differences between the ethnic groups in formation and detoxification of the toxic CPO metabolite, the obtained *in vivo* dose-response curves predicted CPF to be 4- to 7-fold more toxic for the Caucasian than for the Chinese population. This was also reflected by the $ED_{10/20}$ and $ED_{10/20}/3$ values derived from the predicted dose-response curves, being 5- to 6-fold higher for the Chinese than the Caucasian population. Important to note as well is that the predicted-PODs obtained from the present study matches relatively well with the PODs defined previously by both EFSA and EPA in their risk assessment of CPF (BfR, 2012; EFSA, 2014; Fan, 2014; Koshlukova and Reed, 2014).

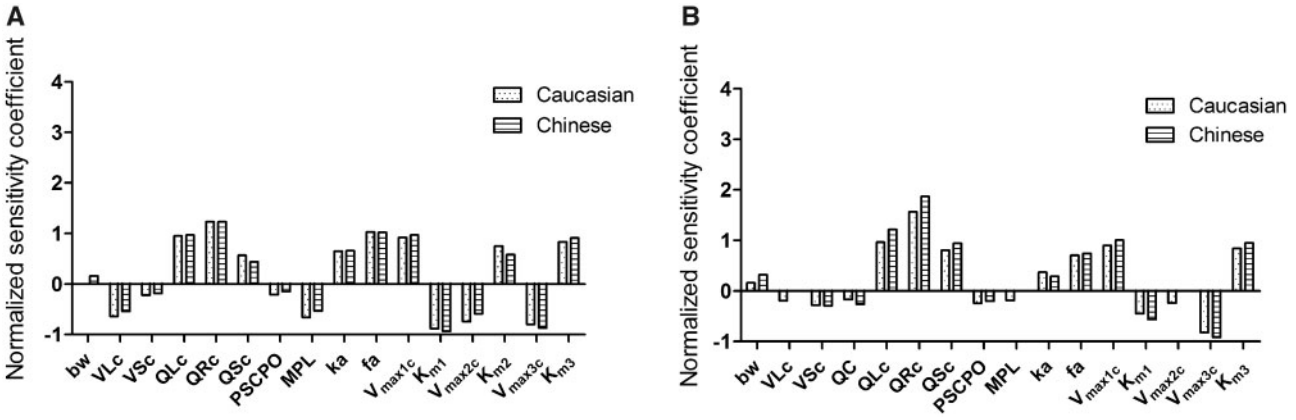

Figure 7. Sensitivity analysis representing the influence of model parameters on the predicted blood C_{max} of CPO in the Caucasian and the Chinese population at a dose of (A) 0.5 mg CPF/kg bw and (B) 180 mg CPF/kg bw. The parameters are stand for bw = body weight, VLc = fraction of liver tissue, VSc = fraction of slowly perfused tissue (bone, skin, and muscle), QC = cardiac output, QLc = fraction of blood flow to liver, QRc = fraction of blood flow to richly perfused tissue, QSc = fraction of blood flow to slowly perfused tissue (bone, skin, and muscle), PSCPO = slowly perfused tissue/blood partition coefficient of CPO, MPL = scaling factor of human liver microsome, ka = absorption constant, fa = fractional absorption, V_{max1c} = maximum rate of conversion from CPF to CPO, K_{m1} = kinetic constant for conversion from CPF to CPO, V_{max2c} = maximum rate of conversion from CPF to TCPy, K_{m2} = kinetic constant for conversion from CPF to TCPy, V_{max3c} = maximum rate of conversion from CPO to TCPy, K_{m3} = kinetic constant for conversion from CPO to TCPy.

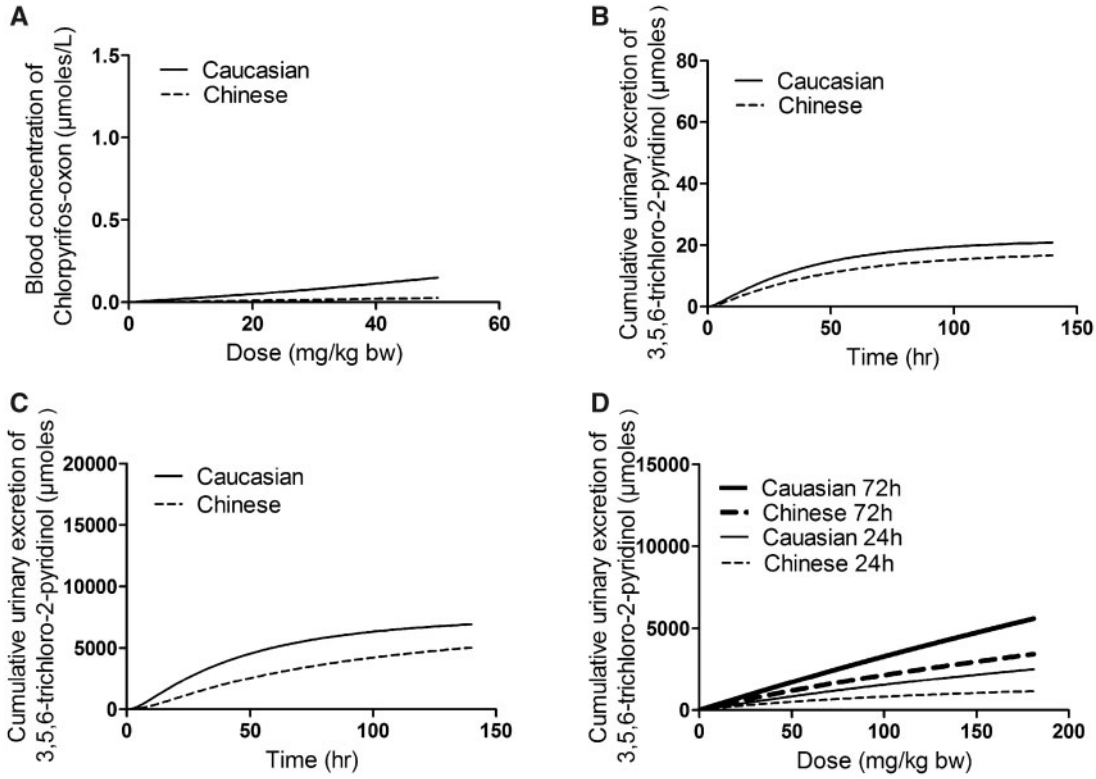

Figure 8. Predicted (A) dose-dependent C_{max} of CPO (B) time-dependent cumulative urinary excretion of TCPy at a dose of 0.5 mg CPF/kg bw, (C) time-dependent cumulative urinary excretion of TCPy at a dose of 180 mg CPF/kg bw, and (D) dose-dependent cumulative urinary excretion of TCPy. All presented for both the Caucasian (solid line) and Chinese (dash line) population, with fa = 0.224 at 24 h (thin solid/dashed line, for (D) only) and 72 h (thick solid/dashed line, for (D) only), respectively (Timchalk *et al.*, 2002).

Although the outcomes of our predictions are considered adequate, the limitations of the approach presented should be considered as well. Thus, it is of importance to mention that the CPO concentration-response curve for RBC AChE inhibition used in the current study was based on data reported by Eyer *et al.* (2009), obtained with blood samples from Sri Lankan patients with acute CPF poisoning (Eyer *et al.*, 2009). In the present study, we assumed that a similar CPO concentration-dependent RBC AChE inhibition would occur in the Chinese and Caucasian individuals, which implies that interethnic differences in AChE sensitivity (if existing) are not (yet) taken into account. However, given the similar primary and tertiary structure of the AChE, it seems likely that interethnic differences in toxicodynamics may be limited, so that the differences

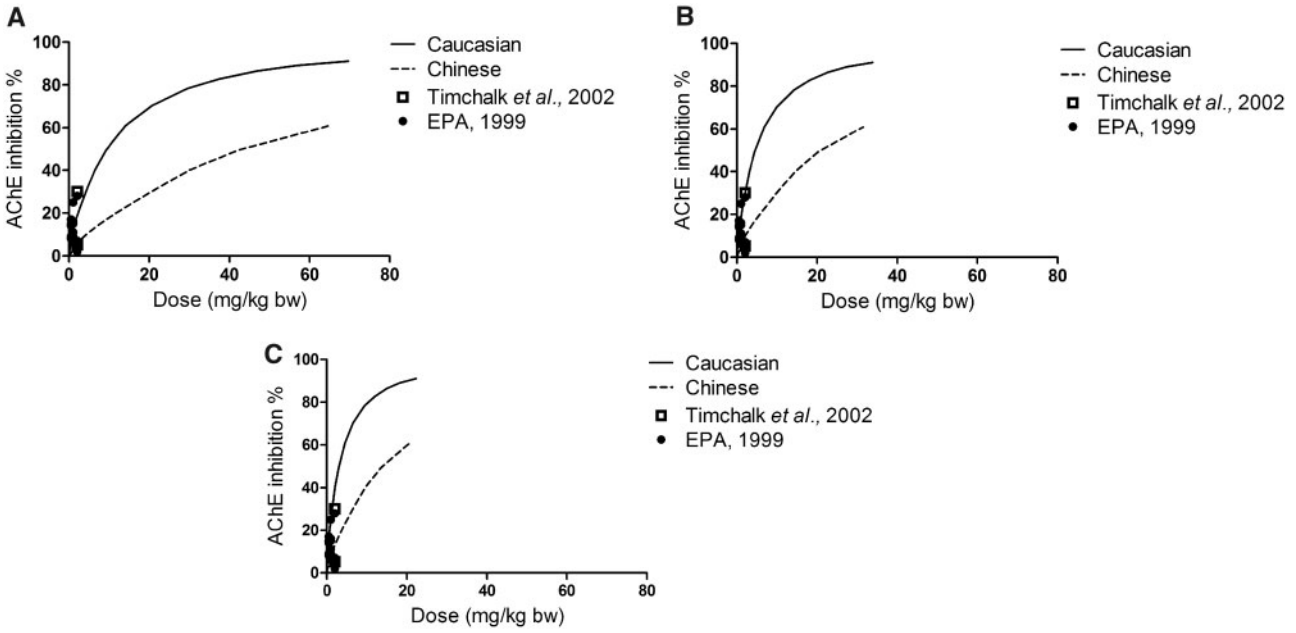

Figure 9. Predicted *in vivo* dose-dependent RBC AChE inhibition upon CPF exposure for the Caucasian (solid line) and Chinese (dash line) population as well as reported data (solid circles/unfilled squares) (EPA, 1999; Timchalk *et al.*, 2002) using (A) fa = 0.224 (Timchalk *et al.*, 2002), (B) fa = 0.46, and (C) fa = 0.70 (Nolan *et al.*, 1984). The solid circles represent the *in vivo* data from humans upon oral administration of 0.5 mg CPF/kg bw, 1 mg CPF/kg bw, and 2 mg CPF/kg bw (EPA, 1999), and the black unfilled square represents *in vivo* data from Timchalk *et al.* (2002) in human exposed to 2 mg CPF/kg bw.

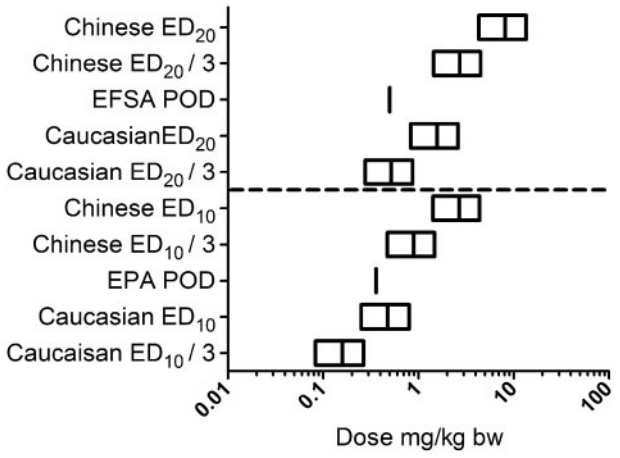

Figure 10. Comparison of the predicted and reported POD values by EFSA (2014) and EPA (BfR, 2012; Fan, 2014; Koshlukova and Reed, 2014) for CPF risk assessment in human. The Y-axis represents the label for the corresponding box plot on the right. The ED_{10} or ED_{20} values represent the predicted effective dose (ED) resulting in 10% or 20% RBC AChE inhibition for the respective populations. The left, middle, and right line in each box plot presents the ED value derived from fa equal to 0.7, 0.462, and 0.224, respectively. The $ED_{10}/3$ or $ED_{20}/3$ values represent PODs derived from these ED values, acknowledging that a BMDL (a lower confidence bound of the BMD) would be accepted as the POD for setting safe levels of exposure when it would be not more than 3-fold lower than the BMD, the dose level resulting in 10% or 20% effect above background level, and thus comparable to the ED. Both ED_{10} and ED_{20} are presented because the cutoff value to set the POD for AChE may be higher than the default of 10%. In this way the predicted values can be compared with the EFSA POD (set at 20% effect level) and EPA POD (set at 10% effect level) (BfR, 2012; Fan, 2014; Koshlukova and Reed, 2014). The dashed line in the plot is separating the results for 20% and 10% effect for RBC AChE inhibition.

in toxicokinetics, as defined in the present study, may have the largest influence on interethnic differences in toxicity. Besides, because the values of kinetic parameters (V_{max4c} and K_{m4} *in vitro*) for PON1-mediated CPO hydrolysis in blood for the Chinese are not available and Chinese plasma samples were not commercially available, this V_{max4c} in μmol/h for the Chinese population was defined by multiplying the value reported by Mosquin *et al.* (2009) in μmol/h/kg $bw^{0.75}$ with the Chinese average body weight 0.75, whereas K_{m4} was kept unchanged. It is important to mention that based on the sensitivity analysis, the impact of V_{max4c} and K_{m4} on the predicted maximum blood concentration of CPO appeared to be quite low (the SCs amount to a value of <0.01 data not shown), which indicates that the impact of PON1-mediated CPO hydrolysis in blood on the predicted maximum blood concentration of CPO appears to be limited if not negligible. This is supported by the fact that a 10-fold change in either V_{max4c} or K_{m4} in the Chinese model did not affect the predicted maximum blood concentration of CPO (Supplementary Data IV).

In conclusion, our developed-CPF PBK models together with reverse dosimetry are capable of predicting the *in vivo* kinetics and biomarker characteristics of CPF as well as CPF exposure related RBC AChE inhibition in human in a quantitative way. By developing the model for both the Chinese and Caucasian population, insight was obtained in the ethnic-related variation in these parameters. The observed interethnic variation in the derived PODs for the 2 populations may be caused by the racial variation in hepatic patterns of the enzymes preferably involved in CPF bioactivation and detoxification, in particular CYP2B6 and PON1, respectively. This variation in enzymes involved may be related to variation in the frequency of relevant SNPs between the Chinese and Caucasian population (Ali and Chia, 2008; Guan *et al.*, 2006; Lamba *et al.*, 2003;). Altogether, it is concluded that the interethnic variation in kinetics of CFP may affect both its biomarker-based exposure assessment and its toxicity and risk assessment, and the developed-CPF PBK models are able to facilitate characterization and quantification of these interethnic differences.

SUPPLEMENTARY DATA

Supplementary data are available at *Toxicological Sciences* online.

DECLARATION OF CONFLICTING INTERESTS

The authors declared no potential conflicts of interest with respect to the research, authorship, and/or publication of this article.

FUNDING

This work was funded by a Grant from the China Scholarship Council (No. 201707720063 to ZHAOSHENSHENG).

REFERENCES

Al-Subeihi, A. A., Spenkelink, B., Punt, A., Boersma, M. G., van Bladeren, P. J., and Rietjens, I. M. C. M. (2012). Physiologically based kinetic modeling of bioactivation and detoxification of the alkenylbenzene methyleugenol in human as compared with rat. *Toxicol. Appl. Pharmacol.* **260**, 271–284.

Al-Malahmeh, A. J., Al-Ajlouni, A., Wesseling, S., Soffers, A. E. M. F., Al-Subeihi, A., Kiwamoto, R., Vervoort, J., and Rietjens, I. M. C. M. (2017). Physiologically based kinetic modeling of the bioactivation of myristicin. *Arch. Toxicol.* **91**, 713–734.

Ali, S. M., and Chia, S. E. (2008). Interethnic variability of plasma paraoxonase (PON1) activity towards organophosphates and PON1 polymorphisms among Asian populations—A short review. *Ind. Health* **46**, 309–317.

Barter, Z. E., Tucker, G. T., and Rowland-Yeo, K. (2013). Differences in cytochrome p450-mediated pharmacokinetics between chinese and caucasian populations predicted by mechanistic physiologically based pharmacokinetic modelling. *Clin. Pharmacokinet.* **52**, 1085–1100.

Barter, Z., Bayliss, M., Beaune, P., Boobis, A., Carlile, D., Edwards, R., Brian Houston, J., Lake, B., Lipscomb, J., Pelkonen, O., *et al.* (2007). Scaling factors for the extrapolation of in vivo metabolic drug clearance from in vitro data: Reaching a consensus on values of human micro-somal protein and hepatocellularity per gram of liver. *Curr. Drug Metab.* **8**, 33–45.

BfR. (2012). Reconsideration of the human toxicological reference values (ARfD, ADI) for chlorpyrifos—BfR opinion No 026/2012, 1 June. Available at: https://www.bfr.bund.de/cm/349/reconsideration-of-the-human-toxicological-reference-values-arfd-adi-for-chlorpyrifos.pdf. Accessed January 23, 2019.

Bouchard, M., Carrier, G., Brunet, R. C., Bonvalot, Y., and Gosselin, N. H. (2005). Determination of biological reference values for chlorpyrifos metabolites in human urine using a toxicokinetic approach. *J. Occup. Environ. Hygiene* **2**, 155–168.

Bouchard, M. F., Chevrier, J., Harley, K. G., Kogut, K., Vedar, M., Calderon, N., Norma, C., Trujillo, C., Johnson, C., Bradman, A., *et al.* (2011). Prenatal exposure to organophosphate pesticides and IQ in 7-year-old children. *Environ. Health Perspect.* **119**, 1189.

Brock, A., and Brock, V. (1990). Plasma cholinesterase activity in a healthy population group with no occupational exposure to known cholinesterase inhibitors: Relative influence of some factors related to normal inter-and intra-individual variations. *Scand. J. Clin. Lab. Investig.* **50**, 401–408.

Brown, R. P., Delp, M. D., Lindstedt, S. L., Rhomberg, L. R., and Beliles, R. P. (1997). Physiological parameter values for physiologically based pharmacokinetic models. *Toxicol. Ind. Health* **13**, 407–484.

Brzak, K. A. (2000). A rising dose toxicology study to determine the no-observable-effect-levels (NOEL) for erythrocyte acetylcholinesterase (AChE) inhibition and cholinergic signs and symptoms of chlorpyrifos at three dose levels œ Part B (Report No 981176). *Toxicology & Environmental Research and Consulting*.

Carr, R. L., Dail, M. B., Chambers, H. W., and Chambers, J. E. (2015). Species differences in paraoxonase mediated hydrolysis of several organophosphorus insecticide metabolites. *J. Toxicol.* **2015**, 1.

DeJongh, J., Verhaar, H. J., and Hermens, J. L. (1997). A quantitative property-property relationship (QPPR) approach to estimate in vitro tissue-blood partition coefficients of organic chemicals in rats and humans. *Arch. Toxicol.* **72**, 17–25.

Di, L., Keefer, C., Scott, D. O., Strelevitz, T. J., Chang, G., Bi, Y. A., Lai, Y., Duckworth, J., Fenner, K., Troutman, M. D., *et al.* (2012). Mechanistic insights from comparing intrinsic clearance values between human liver microsomes and hepatocytes to guide drug design. *Eur. J. Med. Chem.* **57**, 441–448.

Drevenkar, V., Stengl, B., and Fröbe, Z. (1994). Microanalysis of dialkylphosphorus metabolites of organophosphorus pesticides in human blood by capillary gas chromatography and by phosphorus-selective and ion trap detection. *Anal. Chim. Acta* **290**, 277–286.

Eaton, D. L., Daroff, R. B., Autrup, H., Bridges, J., Buffler, P., Costa, L. G., Coyle, J., McKhann, G., Mobley, W. C., Nadel, L., *et al.* (2008). Review of the toxicology of chlorpyrifos with an emphasis on human exposure and neurodevelopment. *Crit. Rev. Toxicol.* **38**, 1–125.

European Food Safety Authority. (2014). Conclusion on the peer review of the pesticide human health risk assessment of the active substance chlorpyrifos. *EFSA J.* **12**, 3640.

EPA. (1999). Data Evaluation Record Study Type: Special Non-Guideline Assessment for RBC Cholinesterase in Humans. Available at: https://archive.epa.gov/scipoly/sap/meetings/web/pdf/kisickider.pdf. Accessed January 23, 2019.

EPA. (2011). Chlorpyrifos Physiologically Based Pharmacokinetic and Pharmacodynamic (PBPK/PD) Modeling Linked to Cumulative and Aggregate Risk Evaluation System (CARES). Available at: https://archive.epa.gov/scipoly/sap/meetings/web/pdf/021511minutes.pdf. Accessed November 1, 2018.

EPA. (2016). Chlorpyrifos: Revised Human Health Risk Assessment for Registration Review. Available at: https://www.regulations.gov/document? D=EPA-HQ-OPP-2015-0653-0454. file ID: EPA-HQ-OPP-2015-0653-0454. Accessed January 23, 2019.

Evans, M. V., and Andersen, M. E. (2000). Sensitivity analysis of a physiological model for 2,3,7,8-tetrachlorodibenzo-p-dioxin (TCDD): Assessing the impact of specific model parameters on sequestration in liver and fat in the rat. *Toxicol. Sci.* **54**, 71–80.

Eyer, F., Roberts, D. M., Buckley, N. A., Eddleston, M., Thiermann, H., Worek, F., and Eyer, P. (2009). Extreme variability in the formation of chlorpyrifos oxon (CPO) in patients poisoned by chlorpyrifos (CPF). *Biochem. Pharmacol.* **78**, 531–537.

Fan, A. M. (2014). Biomarkers in toxicology, risk assessment, and environmental chemical regulations. In *Biomarkers in Toxicology* (pp. 1057–1080). https://doi.org/10.1016/B978-0-12-404630-6.00064-6

Foxenberg, R. J., Ellison, C. A., Knaak, J. B., Ma, C., and Olson, J. R. (2011). Cytochrome P450-specific human PBPK/PD models for the organophosphorus pesticides: Chlorpyrifos and parathion. *Toxicology* **285**, 57–66.

Foxenberg, R. J., McGarrigle, B. P., Knaak, J. B., Kostyniak, P. J., and Olson, J. R. (2007). Human hepatic cytochrome p450-specific metabolism of parathion and chlorpyrifos. *Drug Metab. Dispos.* **35**, 189–193.

Flaskos, J. (2014). The neuronal cytoskeleton as a potential target in the developmental neurotoxicity of organophosphorothionate insecticides. *Basic Clin. Pharmacol. Toxicol.* **115**, 201–208.

Furlong, C. E., Richter, R. J., Seidel, S. L., Costa, L. G., and Motulsky, A. G. (1989). Spectrophotometric assays for the enzymatic hydrolysis of the active metabolites of chlorpyrifos and parathion by plasma paraoxonase/arylesterase. *Anal. Biochem.* **180**, 242–247.

González-Alzaga, B., Lacasaña, M., Aguilar-Garduño, C., Rodríguez-Barranco, M., Ballester, F., Rebagliato, M., and Hernández, A. F. (2014). A systematic review of neurodevelopmental effects of prenatal and postnatal organophosphate pesticide exposure. *Toxicol. Lett.* **230**, 104–121.

Griffin, P., Mason, H., Heywood, K., and Cocker, J. (1999). Oral and dermal absorption of chlorpyrifos: A human volunteer study. *Occup. Environ. Med.* **56**, 10–13.

Guan, S., Huang, M., Li, X., Chen, X., Chan, E., and Zhou, S. F. (2006). Intra-and inter-ethnic differences in the allele frequencies of cytochrome P450 2B6 gene in Chinese. *Pharm. Res.* **23**, 1983–1990.

Hardt, J., and Angerer, J. (2000). Determination of dialkyl phosphates in human urine using gas chromatography-mass spectrometry. *J. Anal. Toxicol.* **24**, 678–684.

Heilmair, R., Eyer, F., and Eyer, P. (2008). Enzyme-based assay for quantification of chlorpyrifos oxon in human plasma. *Toxicol. Lett.* **181**, 19–24.

Hung, D. Z., Yang, H. J., Li, Y. F., Lin, C. L., Chang, S. Y., Sung, F. C., and Tai, S. C. (2015). The long-term effects of organophosphates poisoning as a risk factor of CVDs: A nationwide population-based cohort study. *PLoS One* **10**, e0137632.

Jinno, H., Tanaka-Kagawa, T., Ohno, A., Makino, Y., Matsushima, E., Hanioka, N., and Ando, M. (2003). Functional characterization of cytochrome P450 2B6 allelic variants. *Drug Metab. Dispos.* **31**, 398–403.

Koshlukova, S. E., and Reed, N. R. (2014). Chlorpyrifos. https://doi.org/10.1016/B978-0-12-386454-3.00115-9

Lamba, V., Lamba, J., Yasuda, K., Strom, S., Davila, J., Hancock, M. L., Fackenthal, J. D., Rogan, P. K., Ring, B., Wrighton, S. A., *et al.* (2003). Hepatic CYP2B6 expression: Gender and ethnic differences and relationship to CYP2B6 genotype and CAR (constitutive androstane receptor) expression. *J. Pharmacol. Exp. Ther.* **307**, 906–922.

Lefkowitz, L. J., Kupina, J. M., Hirth, N. L., Henry, R. M., Noland, G. Y., Barbee, J. Y., Zhou, J. Y., and Weese, C. B. (2007). Intraindividual stability of human erythrocyte cholinesterase activity. *Clin. Chem.* **53**, 1358–1363.

Leoni, C., Balduzzi, M., Buratti, F. M., and Testai, E. (2012). The contribution of human small intestine to chlorpyrifos biotransformation. *Toxicol. Lett.* **215**, 42–48.

Liu, P., Wu, C. H., Chang, X. L., Qi, X. J., Zheng, M. L., and Zhou, Z. J. (2014). Assessment of chlorpyrifos exposure and absorbed daily doses among infants living in an agricultural area of the Province of Jiangsu, China. *Int. Arch. Occup. Environ. Health* **87**, 753–762.

Lu, C., Holbrook, C. M., and Andres, L. M. (2009). The implications of using a physiologically based pharmacokinetic (PBPK) model for pesticide risk assessment. *Environ. Health Perspect.* **118**, 125–130.

Mosquin, P. L., Licata, A. C., Liu, B., Sumner, S. C., and Okino, M. S. (2009). Reconstructing exposures from small samples using physiologically based pharmacokinetic models and multiple biomarkers. *J. Exposure Sci. Environ. Epidemiol.* **19**, 284.

Mutch, E., Daly, A. K., and Williams, F. M. (2007). The relationship between PON1 phenotype and PON1-192 genotype in detoxification of three oxons by human liver. *Drug Metab. Dispos.* **35**, 315–320.

Naksen, W., Prapamontol, T., Mangklabruks, A., Chantara, S., Thavornyutikarn, P., Robson, M. G., Ryan, P. B., Barr, D. B., and Panuwet, P. (2016). A single method for detecting 11 organophosphate pesticides in human plasma and breastmilk using GC-FPD. *J. Chromatogr. B* **1025**, 92–104.

NHFPC. (2007a). Reference individuals for use in radiation protection—Part 1: Physique parameters. vol GBZ/T 200.1, Pub. L. No. GBZ/T 200.1. China: National Health and Family Planning Commission of the People's Republic of China. Available at: http://www.nirp.cn/userfiles/file/GBZT200.1-2007.pdf. Accessed January 23, 2019.

NHFPC. (2007b). Reference individuals for use in radiation protection—Part 2: Masses of main organs and tissues.vol GBZ/T 200.2, Pub. L. No. GBZ/T 200.2. China: National Health and Family Planning Commission of the People's Republic of China. Available at: http://www.nirp.cn/userfiles/file/GBZT200.2-2007.pdf. Accessed January 23, 2019.

NHFPC. (2014). Reference individuals for use in radiation protection—Part 3: Main physiological parameters. vol GBZ/T 200.3, Pub. L. No. GBZ/T 200.3. China: National Health and Family Planning Commission of the People's Republic of China. Available at: http://www.nirp.cn/userfiles/file/GBZT200.3-2014.pdf. Accessed January 23, 2019.

Ning, J., Louisse, J., Spenkelink, B., Wesseling, S., and Rietjens, I. M. C. M. (2017). Study on inter-ethnic human differences in bioactivation and detoxification of estragole using physiologically based kinetic modeling. *Arch. Toxicol.* **91**, 3093–3108.

Nolan, R. J., Rick, D. L., Freshour, N. L., and Saunders, J. H. (1984). Chlorpyrifos: Pharmacokinetics in human volunteers. *Toxicol. Appl. Pharmacol.* **73**, 8–15.

Poet, T. S., Kousba, A. A., Dennison, S. L., and Timchalk, C. (2004). Physiologically based pharmacokinetic/pharmacodynamic model for the organophosphorus pesticide diazinon. *Neurotoxicology* **25**, 1013–1030.

Punt, A., Paini, A., Boersma, M. G., Freidig, A. P., Delatour, T., Scholz, G., Schilter, B., Bladeren, P., and Rietjens, I. M. C. M. (2009). Use of physiologically based biokinetic (PBBK) modeling to study estragole bioactivation and detoxification in humans as compared with male rats. *Toxicol. Sci.* **110**, 255–269.

Punt, A., Freidig, A. P., Delatour, T., Scholz, G., Boersma, M. G., Schilter, B., van Bladeren, P. J., and Rietjens, I. M. C. M. (2008). A physiologically based biokinetic (PBBK) model for estragole bioactivation and detoxification in rat. *Toxicol. Appl. Pharmacol.* **231**, 248–259.

Smith, J. N., Timchalk, C., Bartels, M. J., and Poet, T. S. (2011). In vitro age-dependent enzymatic metabolism of chlopyrifos and chlorpyrifos-oxon in human hepatic microsomes as well as chlorpyrifos-oxon in plasma. *Drug Metab. Dispos., Dmd-111* **39**, 1353.

Stauber, J. L., Chariton, A., and Apte, S. (2016). Global change. In *Marine Ecotoxicology* (pp. 273–313). Academic Press. https://doi.org/http://dx.doi.org/10.1016/B978-0-12-803371-5.00010-2

Tang, J., Cao, Y., Rose, R. L., Brimfield, A. A., Dai, D., Goldstein, J. A., and Hodgson, E. (2001). Metabolism of chlorpyrifos by human cytochrome P450 isoforms and human, mouse, and rat liver microsomes. *Drug Metab. Dispos.* **29**, 1201–1204.

Timchalk, C., Nolan, R. J., Mendrala, A. L., Dittenber, D. A., Brzak, K. A., and Mattsson, J. L. (2002). A physiologically based pharmacokinetic and pharmacodynamic (PBPK/PD) model for the organophosphate insecticide chlorpyrifos in rats and humans. *Toxicol. Sci.* **66**, 34–53.

Wagner, D. (1999). Pesticide residues in food. Available at: http://www.bvsde.ops-oms.org/bvsacg/e/cd-cagua/guias/b.parametos/4.BasTox/IPCS/029.ChlorpyrifosIPCS.pdf. Accessed January 23, 2019.

Wang, P., Tian, Y., Wang, X. J., Gao, Y., Shi, R., Wang, G. Q., Hu, G. H., and Shen, X. M. (2012). Organophosphate pesticide exposure and perinatal outcomes in Shanghai, China. *Environ. Int.* **42**, 100–104.

Yang, J., He, M. M., Niu, W., Wrighton, S. A., Li, L., Liu, Y., and Li, C. (2012). Metabolic capabilities of cytochrome P450 enzymes in Chinese liver microsomes compared with those in Caucasian liver microsomes. *Br. J. Clin. Pharmacol.* **73**, 268–284.

Zhang, Y., Han, S., Liang, D., Shi, X., Wang, F., Liu, W., Zhang, L., Chen, L., Gu, Y., and Tian, Y. (2014). Prenatal exposure to organophosphate pesticides and neurobehavioral development of neonates: A birth cohort study in Shenyang, China. *PLoS One* **9**, e88491.

Zhang, Y., Reviriego, J., Lou, Y. Q., Sjöqvist, F., and Bertilsson, L. (1990). Diazepam metabolism in native Chinese poor and extensive hydroxylators of S-mephenytoin: Interethnic differences in comparison with white subjects. *Clin. Pharmacol. Ther.* **48**, 496–502.